

Vibrational spectroscopy of HOD in liquid D_2O . I. Vibrational energy relaxation

Cite as: J. Chem. Phys. **117**, 5827 (2002); <https://doi.org/10.1063/1.1502248>

Submitted: 03 May 2002 . Accepted: 28 June 2002 . Published Online: 04 September 2002

C. P. Lawrence, and J. L. Skinner



View Online



Export Citation

ARTICLES YOU MAY BE INTERESTED IN

Vibrational spectroscopy of HOD in liquid D_2O . II. Infrared line shapes and vibrational Stokes shift

The Journal of Chemical Physics **117**, 8847 (2002); <https://doi.org/10.1063/1.1514652>

Vibrational spectroscopy of HOD in liquid D_2O . III. Spectral diffusion, and hydrogen-bonding and rotational dynamics

The Journal of Chemical Physics **118**, 264 (2003); <https://doi.org/10.1063/1.1525802>

Combined electronic structure/molecular dynamics approach for ultrafast infrared spectroscopy of dilute HOD in liquid H_2O and D_2O

The Journal of Chemical Physics **120**, 8107 (2004); <https://doi.org/10.1063/1.1683072>

Vibrational spectroscopy of HOD in liquid D₂O. I. Vibrational energy relaxation

C. P. Lawrence and J. L. Skinner^{a)}

Theoretical Chemistry Institute and Department of Chemistry, University of Wisconsin, Madison, Wisconsin 53706

(Received 3 May 2002; accepted 28 June 2002)

We present calculations of the vibrational lifetimes for the three fundamentals of HOD in liquid D₂O. The calculations build on the work of Oxtoby and of Rey and Hynes, but also introduce some new ideas, the most important of which is a self-consistent renormalization scheme for determining the system and bath Hamiltonians for a given vibrational state of the HOD molecule. Our result for T_1 for the OH stretch fundamental is 2.7 ps, which is about a factor of 3 larger than the experimental number. We suggest that including solvent vibrations may bring theory in closer agreement with experiment. © 2002 American Institute of Physics. [DOI: 10.1063/1.1502248]

I. INTRODUCTION

Many chemical and biochemical reactions occur in aqueous solution, and the solvent molecules play an essential role in these processes. As such, it is important to develop a detailed understanding of the structure and dynamics of water molecules around solutes, and indeed, of neat liquid water itself.^{1–4} Structurally, much of what is known about water in the condensed phase comes from x-ray and neutron scattering experiments. From these studies it is possible to determine the average distance between pairs of atoms, as well as the average number of hydrogen bonds the molecules form.^{5,6} Dynamic information comes from dielectric relaxation⁷ and nuclear magnetic resonance (NMR)^{8,9} experiments, both of which have been useful especially in determining the time scales for molecular reorientation. Of particular importance for solvation and reaction chemistry, however, is the dynamics of intramolecular and intermolecular energy transfer. Quite recently a number of experimental and theoretical studies on polyatomic molecules in solution have addressed this general issue.^{10–25}

In water at room temperature only the ground vibrational state has appreciable population in thermal equilibrium. If one of the molecules is excited vibrationally, it will relax by transferring its energy, ultimately, to rotational and translational degrees of freedom of both the originally excited molecule and its neighbors. Intermediates along the way, however, may involve different vibrational states of the originally excited molecule, and vibrational excitations on neighboring molecules as well. It is of great interest to map out such relaxation pathways, and to determine the relevant rate constants. An important step in this direction comes from pump–probe vibrational energy relaxation (VER) experiments. A particular vibrational eigenstate is excited initially, and then the population of this state is monitored as a function of time. In favorable situations this population decays exponentially, naturally defining a vibrational lifetime T_1 . Such VER experiments have recently been performed on the

OH stretch of dilute HOD in liquid D₂O at room temperature.^{26–34} This particular combination of isotopes is chosen because in this case the OH stretch is spectrally distinct, and the HOD molecules are dilute so as to avoid resonant vibration–vibration energy transfer. The earliest measurements of T_1 for this system gave conflicting values of about 0.5²⁶ and 8 ps.²⁷ In more recent years, lasers with shorter pulses have allowed for more accurate measurements, and at this point the accepted value for T_1 is about 1 ps.^{28–34} Interestingly, T_1 shows an anomalous temperature dependence in that it increases with increasing temperature.²⁹ T_1 also varies considerably with the frequency of the pump pulse.³¹ We also note that recent elegant infrared pump/Raman probe experiments of Dlott and co-workers³⁴ provide direct information about the relaxation pathways. Most recently, the relaxation time of the OD stretch of dilute HOD in H₂O has been measured to be 1.8 ps.³⁵

Several years ago Rey and Hynes (RH) presented a pioneering, insightful, and detailed theoretical study of the vibrational lifetime of the OH stretch of HOD in D₂O.³⁶ Their basic approach follows Oxtoby,³⁷ where the Hamiltonian for the liquid is partitioned into terms for the vibrations of the HOD molecule (hereafter called the system), the rotations and translations of the HOD molecule and all nuclear degrees of freedom of the D₂O molecules (the bath), and the system–bath interaction. RH used the anharmonic vibrational Hamiltonian for HOD developed by Sceats and Rice,³⁸ and the flexible SPC model for the D₂O solvent.³⁹ The system–bath interaction included potential, Coriolis, and centrifugal coupling. The eigenvalues and eigenstates of the system Hamiltonian were calculated using perturbation theory in the vibrational anharmonicities, and the system–bath interaction was truncated after first order in the vibrational coordinates. RH calculated the rate constants between pairs of vibrational levels using perturbation (Landau–Teller) theory in the system–bath interaction. In this scheme the bath is treated classically, the relevant bath time-correlation functions (TCFs) are computed from a molecular dynamics simulation, and the rate constants are evaluated

^{a)}Electronic mail: skinner@chem.wisc.edu

from Fourier transforms of these TCFs. RH used the “standard” quantum correction factor³⁷ to take into account the fact that the TCFs in the Landau–Teller theory are quantal, whereas those determined from the simulation are classical. They found that one quantum of OH stretch excitation decays in 7.7 ps to the overtone of the HOD bend, which subsequently decays to the bend fundamental, and then to the ground state. Their value of 7.7 ps for T_1 was in good agreement with the accepted experimental value at the time (8 ps),²⁷ but is about one order of magnitude larger than the currently accepted experimental value.^{28–34}

In this paper we present a similar theoretical study. While our approach is very close in spirit to the work of RH,³⁶ there are several significant differences. First of all, the Scaats–Rice³⁸ Hamiltonian used by RH for the HOD vibrations is quartic in the stretching coordinates, quadratic in the bend, and the coupling between the vibrational modes is bilinear. After their work was completed a significantly more accurate vibrational Hamiltonian became available,⁴⁰ which treats the anharmonic interactions and mode couplings to high order. The many parameters of the Hamiltonian are chosen so its eigenvalues reproduce (to less than a cm^{-1}) over three thousand rotation–vibration energies for gas-phase H_2^{16}O . In our work we use this Hamiltonian. RH used perturbation theory (in the cubic and quartic anharmonicities) to determine the eigenvalues and eigenstates. We have found (for both Hamiltonians) that it is substantially more accurate to determine the eigenvalues and eigenstates exactly (by diagonalizing the matrix using a product harmonic basis set), which is how we proceed herein. The RH (Scaats–Rice) Hamiltonian has an adjustable parameter for the stretch force constants so that the frequencies can be shifted from those appropriate for the gas phase molecule to those appropriate for the liquid. In contrast, we determine the frequency shifts from the gas phase self-consistently (see below) from the interactions of the HOD molecule with the D_2O solvent. As mentioned above, when calculating the system–bath interaction RH kept all terms to linear order in the normal mode coordinates. We find that in fact the Taylor series does not converge until at least second, if not third, order, and so we keep terms up to third order herein. RH considered three contributions (potential, Coriolis, and centrifugal) to the system–bath interactions. In calculating the relevant TCFs RH neglected cross terms between these contributions. We find that it is important to include these (especially the potential–Coriolis) cross terms. Quite recently there has been considerable discussion^{41–48} about the appropriate form for the quantum correction factor.^{37,42,49,50} Most people (including RH) until very recently have been using the “standard” quantum correction factor, proposed by Oxtoby³⁷ and others some time ago. However, we have found,^{45,46,48} by considering exactly solvable model problems, that depending on the nature of the problem, other (of course still approximate) forms are more appropriate. These forms have been implemented in calculations of VER for realistic models of liquid diatomics.^{46,51–53} In the present study the harmonic–Schofield quantum correction factor is used, which we believe is more accurate than the standard factor for the case at hand.⁴⁶

A novel feature of our work is that we determine certain

parameters of the bath Hamiltonian self-consistently for a given vibrational state of the HOD molecule. Traditionally the bath Hamiltonian is taken to be independent of the solute’s vibrational state, and indeed, there is every indication that in most instances this is an excellent approximation. Note, however, that for any vibrational transition this approximation leads to the absence of a Stokes shift (the difference between the average transition frequency in absorption and (relaxed) emission). Remarkably, a Stokes shift of 70 cm^{-1} was recently measured for the system under consideration!⁵⁴ Evidently, then, for water (presumably because of very strong hydrogen-bonding interactions) the bath Hamiltonian does depend substantially on the vibrational state of the HOD. To incorporate this effect in our theory, we first include the average system–bath interaction in the system Hamiltonian. The solute’s atomic positions (expectations values of the vibrational coordinates in a given vibrational state) are then determined. These new positions modify the bath Hamiltonian (since the bath involves the translational and rotational coordinates of *all* molecules). The bath average of the system–bath interaction is then determined again, and the process is iterated until convergence is obtained, at which point the system and bath Hamiltonians have been determined self-consistently, for a given vibrational state. In this manner the average frequency shifts from the gas phase are incorporated into the system Hamiltonian. For the VER problem, the appropriate vibrational state is the one that is initially excited, in this case the state with one quantum of OH stretch.

Our theory produces a value of 2.7 ps for T_1 , which is about three times longer than the experimental value. We find, as did RH before us, that the primary pathway is via relaxation to the overtone of the bend. We have also calculated T_1 following excitation of the OD stretch fundamental, and the bend fundamental (of HOD in D_2O). The results are 18 ps and 220 fs, respectively, and the dominant pathways involve, respectively, transitions to the bend fundamental and to the ground state. Note that while the former cannot be measured experimentally because the OD stretch of HOD could not be resolved from that of the solvent, the latter is in principle experimentally accessible, but has not yet been measured because of the unavailability of tunable ultrafast lasers of low enough frequency.

The organization of this paper is as follows. The Hamiltonian for the HOD– D_2O system is described in Sec. II, as is our renormalization procedure for determining the system and bath self-consistently for a given vibrational state. Section III outlines the method by which T_1 is calculated. In Sec. IV, we present T_1 results for relaxation from each of the HOD fundamentals. In addition, the most important step in the relaxation of the OH stretch fundamental (the transition to bend overtone) is broken down into its various contributions. In Sec. V, we discuss how inclusion of solvent vibrations might well decrease our theoretical values of T_1 . We also discuss our results in light of previous experimental studies. Finally, we mention several direct extensions of this work that we intend to pursue, and also discuss related theoretical work in progress on the same system.

II. HAMILTONIAN

As discussed in the Introduction, we begin by writing the Hamiltonian as a sum of contributions from the isolated HOD molecule, the (liquid) D₂O solvent, and the HOD–D₂O interaction. These are each discussed in turn below. We end this section by rewriting the Hamiltonian as a sum of terms for the HOD vibrations (the system), all the molecular rotations and translations (the bath), and the system–bath interaction. We also describe our self-consistent renormalization scheme for determining the appropriate system and bath Hamiltonians for a given vibrational state of the system.

A. Isolated HOD

To describe the vibrational degrees of freedom of the HOD molecule we begin with the potential energy surface, V_{vib} , for H₂¹⁶O described by Polyansky *et al.*⁴⁰ This highly accurate potential includes coupling among the three anharmonic vibrational modes of water. Using this potential, Polyansky *et al.* calculated the energies of 3200 experimentally observed rotation–vibration levels, finding a standard deviation of 0.6 cm^{−1}. V_{vib} is expressed in terms of the bond-stretching coordinates, $\Delta r_1 = r_1 - r_1^e$ and $\Delta r_3 = r_3 - r_3^e$ (where r_1 and r_3 are the two bond lengths and r_1^e and r_3^e are their equilibrium values), and the supplement of the bond angle ρ (with equilibrium value ρ_e)

$$\begin{aligned} V_{\text{vib}}(\Delta r_1, \Delta r_3, \rho) \\ = V_0(\rho) + \sum_j F_j(\rho) y_j + \sum_{j \leq k} F_{jk}(\rho) y_j y_k \\ + \sum_{j \leq k \leq m} F_{jkm}(\rho) y_j y_k y_m \\ + \sum_{j \leq k \leq m \leq n} F_{jkmn}(\rho) y_j y_k y_m y_n + f_{11111}(y_1^5 + y_3^5) \\ + f_{111111}(y_1^6 + y_3^6) + f_{1111111}(y_1^7 + y_3^7), \end{aligned} \quad (1)$$

where $j, k, m, n = 1$ or 3

$$y_j = 1 - \exp(-a_j \Delta r_j), \quad (2)$$

$$V_0(\rho) = \sum_{i=2}^{12} f_0^{(i)} (\cos \rho_e - \cos \rho)^i, \quad (3)$$

$$F_j(\rho) = \sum_{i=1}^4 f_j^{(i)} (\cos \rho_e - \cos \rho)^i, \quad (4)$$

$$F_{jk\dots}(\rho) = f_{jk\dots}^{(0)} + \sum_{i=1}^N f_{jk\dots}^{(i)} (\cos \rho_e - \cos \rho)^i. \quad (5)$$

The functions $F_{jk}(\rho)$, $F_{jkl}(\rho)$, and $F_{jklm}(\rho)$ have $N=3$, 2 , and 1 , respectively. For the values of the constants in the above expressions, see Ref. 40. Within the Born–Oppenheimer approximation the potential is independent of the nuclear isotopes, and so we use this same potential for HOD. In what follows it will be convenient to transform from internal coordinates to dimensionless normal coordinates. To this end, first the internal coordinates are expressed in Cartesian displacement coordinates for each of the atoms,

through a nonlinear transformation. Then the normal coordinates are defined in terms of the Cartesian displacement coordinates by truncating the potential at second order and applying the FG matrix method of Wilson, Decius, and Cross.⁵⁵

The kinetic energy of the isolated HOD molecule is given by⁵⁶

$$\begin{aligned} T = \frac{1}{2} \sum_{\alpha\beta} (L_\alpha - \pi_\alpha) \mu_{\alpha\beta} (L_\beta - \pi_\beta) \\ + \frac{1}{2} \sum_s \hbar \omega_s p_s^2 - \frac{\hbar^2}{8} \sum_\alpha \mu_{\alpha\alpha} + \frac{P_c^2}{2M_c}. \end{aligned} \quad (6)$$

α (and β) label the molecule's three principal axes, L_α is the angular momentum about axis α , and $\mu_{\alpha\beta}$ are the elements of the effective reciprocal inertia tensor. π_α is often referred to as the vibrational angular momentum, which is given by

$$\pi_\alpha = \hbar \sum_{ss'} \frac{\omega_{s'}}{\omega_s} \zeta_{ss'}^{(\alpha)} q_s p_{s'}, \quad (7)$$

where $\zeta_{ss'}^{(\alpha)}$ is a geometric parameter, q_s is the dimensionless vibrational normal coordinate for mode s , p_s is its conjugate momentum, and ω_s is the harmonic frequency of that mode. This form of the kinetic energy was first described by Watson in 1968,⁵⁶ greatly simplifying the vibration–rotation Hamiltonian of Darling and Dennison.⁵⁷ The term $-(\hbar^2/8) \sum_\alpha \mu_{\alpha\alpha}$ is often referred to as the Watson term. P_c is the linear momentum and M_c is the mass of the HOD molecule. Initially, the Hamiltonian will be treated in the absence of translational and rotational energy ($P_c, L_\alpha = 0$), as these variables will be treated classically (see below). The sum of the remaining kinetic energy terms and the potential energy will be denoted as H_{vib}

$$H_{\text{vib}} = \frac{1}{2} \sum_{\alpha\beta} \pi_\alpha \mu_{\alpha\beta} \pi_\beta + \frac{1}{2} \sum_s \hbar \omega_s p_s^2 - \frac{\hbar^2}{8} \sum_\alpha \mu_{\alpha\alpha} + V_{\text{vib}}. \quad (8)$$

To find the eigenvalues and eigenfunctions of H_{vib} , we diagonalize it using a basis set of uncoupled harmonic oscillators for the three vibrational modes. In these calculations the Hamiltonian is expressed as a Taylor series in the normal mode coordinates, which is truncated such that the sum of the powers for the three coordinates is less than or equal to 14. $\mu_{\alpha\beta}$ are expanded up to fourth order in the normal mode coordinates. The basis set consisted of harmonic oscillator product states of up to 10 quanta for each of the oscillators. Comparing a few of the lowest energy states for H₂¹⁶O to those calculated by Polyansky *et al.*,⁴⁰ the greatest difference was about 0.5 cm^{−1}. This difference presumably results from differences in the choice of coordinate systems and basis functions. We have also performed the analogous calculations for HOD, and we again satisfactorily reproduce the experimentally observed energy levels.⁵⁸

Now considering $P_c \neq 0$, $L_\alpha \neq 0$, the additional contributions to the kinetic energy will be grouped into three terms: Translational, centrifugal, and Coriolis. The translational energy is given trivially as

$$T_{\text{tr}} = \frac{P_c^2}{2M_c}. \quad (9)$$

The Coriolis term includes those parts of the Hamiltonian that couple the components of the angular momentum to the vibrational angular momenta

$$T_{\text{Cor}} = -\frac{1}{2} \sum_{\alpha\beta} (L_\alpha \mu_{\alpha\beta} \pi_\beta + \pi_\alpha \mu_{\alpha\beta} L_\beta). \quad (10)$$

In fact Watson⁵⁶ showed that $[\pi_\alpha, \mu_{\alpha\beta}] = 0$, which means that the two terms in the above equation are equal. Furthermore, for a planar molecule (such as water), this reduces to³⁶

$$T_{\text{Cor}} = -L_z \mu_{zz} \pi_z, \quad (11)$$

where z is the out-of-plane axis. The remaining terms give the centrifugal contribution

$$T_{\text{cen}} = \frac{1}{2} \sum_{\alpha\beta} L_\alpha \mu_{\alpha\beta} L_\beta. \quad (12)$$

Thus, the Hamiltonian for the isolated HOD molecule is given by

$$H_{\text{iso}} = T + V_{\text{vib}} = H_{\text{vib}} + T_{\text{tr}} + T_{\text{Cor}} + T_{\text{cen}}. \quad (13)$$

H_{vib} involves only the vibrations of the HOD molecule, T_{tr} involves only the center-of-mass translations, and T_{Cor} and T_{cen} couple the molecule's rotations and vibrations (recall that $\mu_{\alpha\beta}$ depend on the normal mode coordinates).

B. D₂O

The intermolecular potential of the N solvent molecules is described by the TIP4P model.⁵⁹ This is a rigid four-site model that includes a combination of Lennard-Jones and Coulomb interactions. Each molecule has a single Lennard-Jones site placed on the oxygen atom. Positive charges are then attached to the hydrogen (or, in this case, deuterium) atoms, and a complementary negative charge is placed on a fourth site, which lies on the symmetry axis of the molecule, in between the oxygen and deuterium atoms. The total energy for the solvent molecules is written

$$H_{\text{sol}} = \sum_{i=1}^N \left(\frac{P_i^2}{2M} + \sum_{\alpha} \frac{L_{\alpha i}^2}{2I_{\alpha}} \right) + \frac{1}{2} \sum_{i \neq j} \left[4\epsilon \left\{ \left(\frac{\sigma}{r_{ij}} \right)^{12} - \left(\frac{\sigma}{r_{ij}} \right)^6 \right\} + \frac{1}{4\pi\epsilon_0} \sum_{m,n} \frac{Q_i^m Q_j^n}{r_{ij}^{mn}} \right]. \quad (14)$$

In this equation, P_i is the linear momentum and $L_{\alpha i}$ is the angular momentum for axis α of molecule i . M is the D₂O mass and I_{α} is the moment of inertia for axis α . ϵ and σ are the Lennard-Jones parameters and r_{ij} is the distance between the Lennard-Jones sites for molecules i and j . Q_i^m is the charge for site m on molecule i and r_{ij}^{mn} is the distance between charge sites for two interacting solvent molecules.

C. HOD in D₂O

The interaction of the HOD molecule with the D₂O solvent is treated in the same manner as the solvent-solvent interaction described above. A single Lennard-Jones site is

placed on the oxygen atom of HOD, with the same parameters as the TIP4P model. Equal positive charges are placed on both the H and D atoms, with a corresponding negative charge on the fourth TIP4P site. The choice of charges for the atoms is discussed in the following subsection. The form of the potential for these interactions is the same as that of the solvent molecules

$$H_{\text{int}} = \sum_{j=1}^N \left[4\epsilon \left\{ \left(\frac{\sigma}{r_{cj}} \right)^{12} - \left(\frac{\sigma}{r_{cj}} \right)^6 \right\} + \frac{1}{4\pi\epsilon_0} \sum_{m,n} \frac{Q_c^m Q_j^n}{r_{cj}^{mn}} \right], \quad (15)$$

where r_{cj} and r_{cj}^{mn} are the distances between the Lennard-Jones and charge sites m and n for the HOD molecule and molecule j , respectively. Q_c^m is the charge of site m on HOD. H_{int} depends on the rotational and translational coordinates of all the molecules, as well as on the normal coordinates of the HOD molecule, since all the distances between sites are functions of these coordinates. Also note that we assume that the fourth TIP4P site on the HOD molecule is rigidly attached to the oxygen atom, in the sense that in the molecule's body-fixed frame the Cartesian displacements of these two sites (as a result of normal coordinate displacements) are identical.

D. Self-consistent renormalization procedure

As a first step we organize the total Hamiltonian in a more useful form. Summing the contributions described above, we have

$$H = H_{\text{iso}} + H_{\text{sol}} + H_{\text{int}} \\ = H_{\text{vib}} + H_{\text{sol}} + T_{\text{tr}} + T_{\text{cen}} + H_{\text{int}} + T_{\text{Cor}}. \quad (16)$$

Normally one would then define the quantum-mechanical "system" Hamiltonian, $H_s \equiv H_{\text{vib}}$, which depends only on the vibrational coordinates and momenta. It has a set of eigenvalues and eigenstates: $H_s|i\rangle = E_i|i\rangle$, $i=0,1,2,\dots$. The "bath" Hamiltonian, H_b , which depends only on translational and rotational coordinates (of all the molecules), is $H_{\text{sol}} + T_{\text{tr}}$ plus T_{cen} and H_{int} evaluated at $\mathbf{q}=0$, where \mathbf{q} is the set of three q_s . (Note that T_{Cor} evaluated at $\mathbf{q}=0$ is zero, and so this term is not included in the bath.) Finally, the system-bath interaction, V , is $T_{\text{cen}} + H_{\text{int}} + T_{\text{Cor}}$ minus the former two terms evaluated at $\mathbf{q}=0$. The bath is treated classically, and so V involves both quantum-mechanical system operators and classical bath variables.

As discussed in the Introduction, for our problem (and especially for the calculation of the vibrational Stokes shift in paper II of this series⁶⁰) it is important that the bath depends on which vibrational state the system is in. Therefore, assuming that the HOD molecule is in vibrational state l , instead of including in the bath the contributions of T_{cen} and H_{int} evaluated at $\mathbf{q}=0$, here we evaluate these terms at $\mathbf{q} = \mathbf{q}_l = \langle l|\mathbf{q}|l\rangle$. Thus, for the bath Hamiltonian, the atomic positions of HOD are determined from these coordinate expectation values for vibrational state l . For a nearly harmonic system, these matrix elements would be approximately equal to zero, so this distinction would make little difference. However, for a strongly anharmonic system such as water, this difference is quite significant. As such, in this treatment the terms in the bath Hamiltonian will be evaluated at \mathbf{q}

$=q_{ll}$. Note that in principle now the Coriolis term could contribute to the bath, since it is nonzero when evaluated at q_{ll} and p_{ll} . However, it is also imaginary! Not quite knowing how to deal with an imaginary term in the bath Hamiltonian, instead we leave the Coriolis term in the system–bath interaction. Thus we have

$$H = H_s + H_b + V, \quad (17)$$

$$H_s = H_{\text{vib}}, \quad (18)$$

$$H_b = H_{\text{sol}} + T_{\text{tr}} + T_{\text{cen}}|_{q=q_{ll}} + H_{\text{int}}|_{q=q_{ll}}, \quad (19)$$

$$V = T_{\text{cen}} - T_{\text{cen}}|_{q=q_{ll}} + H_{\text{int}} - H_{\text{int}}|_{q=q_{ll}} + T_{\text{Cor}}. \quad (20)$$

Three of the five terms in V depend on both system operators and bath variables. In what follows it will be convenient to express them as sums of products of system operators and bath variables. To this end T_{cen} and H_{int} are expanded in powers of the normal coordinates around the point $q=0$, keeping all terms up to third order. [Note that as long as we keep enough terms it does not matter about which point we expand, and for convenience in taking matrix elements (see below) we choose to expand around $q=0$.] Similarly, T_{Cor} is expanded to third order in the normal coordinates and conjugate momenta.

In what follows we will be treating V with perturbation theory. In cases where V is not necessarily so small, one can have more confidence in this perturbative approach by adding the bath average of V , $\langle V \rangle_b$ (which is a system operator), to the system Hamiltonian, and then subtracting it from V . Thus

$$H'_s = H_s + \langle V \rangle_b, \quad (21)$$

$$V' = V - \langle V \rangle_b. \quad (22)$$

In this way at least the *bath average* of the perturbation is zero. Note that when the bath average of V is evaluated, terms that are not system operators, such as $T_{\text{cen}}|_{q=q_{ll}}$, need not be included, as these result only in a constant energy shift. The bath average of T_{Cor} is also excluded as this term is proportional to $\langle L_z \rangle_b$. While the use of periodic boundary conditions results in a small nonzero value for this quantity,⁶¹ it is excluded on the basis that for an infinite system it should be exactly zero.

Now we have the interesting situation where the renormalized system Hamiltonian depends on the definition of the bath (through the bath average of V), whereas the bath Hamiltonian depends on the system (through the matrix elements q_{ll} , which are the positions of the HOD atoms for vibrational state l). Therefore, we solve this problem self-consistently by iteration for a given choice of vibrational state l . Initially, the bath is defined by Eq. (19), using the eigenstates of the isolated molecule to evaluate q_{ll} . A molecular-dynamics simulation is then performed, in which the dynamics are propagated with this bath Hamiltonian, and $\langle V \rangle_b$ is evaluated. This term is then included in the system Hamiltonian, as per Eq. (21). The eigenstates of this new system Hamiltonian, H'_s , are used to recalculate q_{ll} , defining a new bath, which is used to evaluate $\langle V' \rangle_b$, and this process is repeated until convergence is reached.

At this point we can discuss the choice of the charge parameters for the HOD molecule. We could simply take the TIP4P values. In this case the interaction between the HOD and D₂O molecules is different from that between the D₂O molecules themselves for two reasons: (1) The equilibrium bond length and angles are slightly different for the Polyan-sky model of HOD and the TIP4P model of D₂O; and (2) for HOD in the ground vibrational state the atomic positions differ from their equilibrium values because of anharmonicities in the HOD potential. So, actually, no matter what charges we assign to the HOD atoms we necessarily have HOD and D₂O molecules that interact differently. Our approach is to choose the charges on the HOD molecule such that the structure of the D₂O fluid [as measured by $g_{\text{OO}}(r)$] around ground-state HOD reproduces as closely as possible the structure of neat TIP4P D₂O (or H₂O). Thus, for a given charge on the H and D atoms, we apply the self-consistent renormalization procedure described above for the *ground* vibrational state of HOD. We then compare the resulting O–O radial distribution function for HOD–D₂O to that for D₂O, repeating the entire procedure with different charges until we get the best agreement.

III. CALCULATION OF T_1

The usual procedure^{20,24,36,37,62,63} for calculating T_1 involves writing the Hamiltonian (which is formally still fully quantum-mechanical) as in Eq. (17). It should be emphasized again, however, that because of the self-consistent renormalization formalism presented herein, H_s and its eigenvalues and eigenstates actually depend on which vibrational state the HOD molecule is in. In a VER experiment the HOD molecule is excited to some vibrational state $l \neq 0$, which, assuming the bath relaxes to this state in a time short compared to the VER time, is then the state for which one performs the self-consistent renormalization. As long as there is not significant back transfer to state l , the rate at which the population of state l changes is simply given by

$$\dot{P}_l(t) = - \sum_{j \neq l} k_{lj} P_l(t), \quad (23)$$

which naturally defines the vibrational lifetime

$$\frac{1}{T_1} \equiv \sum_{j \neq l} k_{lj}. \quad (24)$$

k_{lj} is the rate constant for the transition from state l to state j .

The rate constants k_{lj} can be obtained using Fermi's golden rule³⁷

$$k_{lj} = \frac{1}{\hbar^2} \int_{-\infty}^{\infty} dt e^{i\omega_{lj}t} \langle V_{lj}(t) V_{lj}^\dagger(0) \rangle_b, \quad (25)$$

where $\omega_{lj} = (E_l - E_j)/\hbar$, $V_{lj} = \langle l | V | j \rangle$ and $V_{lj}(t) = e^{iH_b t/\hbar} V_{lj} e^{-iH_b t/\hbar}$. V_{lj} is of course an operator in the bath Hilbert space, and $\langle V_{lj}(t) V_{lj}^\dagger(0) \rangle_b$ is a quantum-mechanical TCF, defined by

$$\langle V_{lj}(t) V_{lj}^\dagger(0) \rangle_b \equiv \text{Tr}_b [\rho_b V_{lj}(t) V_{lj}^\dagger(0)], \quad (26)$$

where

$$\rho_b = e^{-\beta H_b / T} r_b [e^{-\beta H_b}]. \quad (27)$$

The usual approximation is then to replace the Fourier transform of the quantum-mechanical TCF by the Fourier transform of its classical counterpart

$$C_{lj}(t) = \langle V_{lj}(t) V_{lj}^*(0) \rangle_{cl}, \quad (28)$$

multiplied by the so-called quantum correction factor (QCF), $Q(\omega_{lj})$

$$k_{lj} = \frac{Q(\omega_{lj})}{\hbar^2} \hat{C}_{lj}(\omega_{lj}), \quad (29)$$

where

$$\hat{C}_{lj}(\omega) = \int_{-\infty}^{\infty} dt e^{i\omega t} C_{lj}(t). \quad (30)$$

This approach has the great advantage that one can calculate $C_{lj}(t)$ from a classical molecular-dynamics simulation. Multiplication by the QCF is necessary, especially at high frequencies compared to kT , since it is known from exact solutions to model problems that the Fourier transform of the classical TCF can severely underestimate (by orders of magnitude) the Fourier transform of the quantum TCF.⁴⁶ For a given problem the appropriate form for the QCF is not very clear. At the very least it should obey the property of detailed balance: $Q(-\omega) = e^{-\beta \hbar \omega} Q(\omega)$. Even so, there are an infinite number of choices.^{37,41,42,46,48-50} In this work we use the harmonic/Schofield QCF^{46,48}

$$Q(\omega) = e^{\beta \hbar \omega / 4} \left(\frac{\beta \hbar \omega}{1 - e^{-\beta \hbar \omega}} \right)^{1/2}. \quad (31)$$

This QCF performs well for a model system involving multiphonon relaxation.⁴⁶ Inasmuch as vibrational relaxation in the present problem may involve the excitation of several quanta of low-frequency hindered translations and librations, using this QCF herein seems appropriate. This QCF has also been applied successfully to VER in liquid oxygen and nitrogen.^{46,51,53}

Before concluding this section we note that usually the classical bath variable V_{lj} is real, so that the classical TCF $C_{lj}(t)$ is real (and is also an even function of time). (The same is true if V_{lj} is purely imaginary.) This renders $\hat{C}_{lj}(\omega)$ a real even function of frequency. In our case, however, V_{lj} is complex (the imaginary part comes from the Coriolis interaction). This means that $C_{lj}(t)$ is also complex, the imaginary part coming from the cross terms between the Coriolis and other contributions to V . Nonetheless, this classical TCF has the important symmetry that $C_{lj}(t)^* = C_{lj}(-t)$, with the consequence that $\hat{C}_{lj}(\omega)$ is a real (although not even) function of frequency. Also note that in the more usual case where the bath and system do not depend on vibrational state, $C_{ji}(t) = C_{lj}(t)^*$ (since V is Hermitian), and $\omega_{ji} = -\omega_{lj}$. This means [from Eq. (29)] that $k_{ji} = e^{-\beta \hbar \omega_{lj}} k_{lj}$, which is the usual detailed-balance relation for rate constants in the weak-coupling master equation. In our case, however, because the bath and system do depend on the initial vibrational state, $C_{ji}(t) \neq C_{lj}(t)^*$, $\omega_{ji} \neq -\omega_{lj}$, and so the simple detailed-balance relation is not satisfied. This is not a fundamental flaw with our approach; rather, it is simply a conse-

quence of the fact that when one is not in the weak-coupling limit (an example of which is when the system and bath depend on the initial vibrational state), the equilibrium state of the master equation is more complicated. We will discuss this issue more fully in later work, where we will solve the full vibrational master equation in order to deduce complete intramolecular relaxation pathways.

IV. RESULTS

Our molecular dynamics simulations involved 107 rigid D₂O molecules and one rigid HOD molecule, as described by the bath Hamiltonian. Cubic periodic boundary conditions were applied, where the size of the box was chosen such that the molecular density is the same as the experimental value for D₂O at 300 K, which is $3.32 \times 10^{28} \text{ m}^{-3}$.² The electrostatic forces were calculated using an approximation to the Ewald sum, as described by Adams and Dubey.⁶⁴ The equations of motion were integrated using the leapfrog algorithm with a time step of 1 fs, and the rotational degrees of freedom were treated using quaternions.^{61,65} The system was first equilibrated by periodically rescaling the velocities of the molecules. This continued until the temperature reached the desired value of 300 K, and was maintained to within ± 1 K for 80 ps without adjustment. A subsequent run of between 2 and 10 ns was carried out, during which the quantities of interest were evaluated.

Initially, the self-consistent renormalization procedure described in Sec. III was implemented for the ground vibrational state, in order to determine the best charge parameter to be used for the HOD molecule. With a charge on the hydrogen (and deuterium) of $0.484 e$ we found good agreement between $g_{\text{OO}}(r)$ for HOD-D₂O compared with that for neat TIP4P D₂O. These two radial distribution functions are shown in Fig. 1. For this value of the charge, convergence of the self-consistent renormalization procedure was obtained after four iterations. As discussed earlier, this charge does differ from that ($0.52e$) for TIP4P water.

The self-consistent renormalization procedure was then implemented for the first excited state of the OH stretch, in order to calculate T_1 from this state. After convergence the eigenvalues of H_s were obtained, and these are shown in Fig. 2. For comparison we also show the eigenvalues for the isolated HOD molecule. The label $|ijk\rangle$ corresponds roughly to i

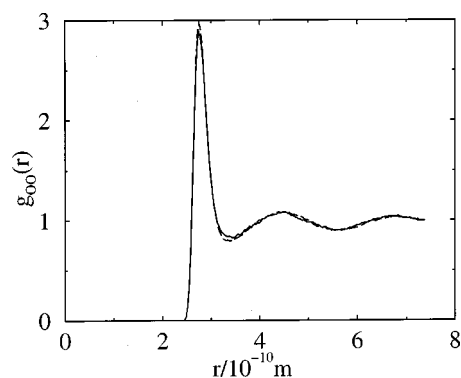


FIG. 1. Oxygen-oxygen radial distribution functions for HOD-D₂O (dashed line) and TIP4P water (solid line).

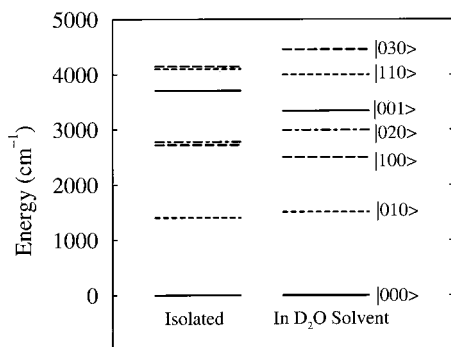


FIG. 2. Vibrational energy levels for the isolated HOD molecule, and for the molecule with one quantum of OH stretch in the D₂O solvent.

quanta of OD stretch, j quanta of bend, and k quanta of OH stretch. We will also label these states in order of increasing energy with $l=0,1,\dots,6$. The OH stretch fundamental corresponds to $l=4$. One sees that the energy level of each vibrational state is shifted very significantly from its gas phase value. (Similar shifts, but for the case when the HOD molecule is in its ground vibrational state, are manifested as solvent shifts in the HOD infrared absorption spectrum, and will be discussed and compared with experiment in paper II of this series.⁶⁰) The transition rate constants from the OH stretch fundamental were calculated using Eq. (29) and computing the classical TCFs $C_{4j}(t)$ from the simulation, for all the states $j \neq 4$ in Fig. 2. The Fourier transforms were evaluated using the Wiener–Khinchine theorem, applying a Hanning window.^{66,67} The results for the rate constants k_{4j} , as well as the frequencies ω_{4j} , are shown in Table I. T_1 was calculated from Eq. (24), with the result of 2.7 ps.

It is seen that the largest rate constant in Table I is for the transition to the bend overtone ($j=3$), although the transitions to the bend and OD stretch fundamentals as well as the ground state also make significant contributions. Focusing on the transition to the bend overtone, $C_{43}(t)$ is shown in Fig. 3. The initial decay of the real part is very fast (about 50 fs), followed by a pronounced beat with a period of about 130 fs, and a slower decay of perhaps 750 fs. The amplitude of the imaginary part is very small, it oscillates with a period of about 70 fs, and decays quickly thereafter.

To understand these time scales, especially of the oscillations, the normalized TCFs of the (vector) linear and angular velocities for the D₂O and HOD molecules were calculated and are shown in Fig. 4. The HOD angular velocity TCF shows an oscillation with a period of about 70 fs, indicating a libration. The D₂O angular velocity TCF shows a

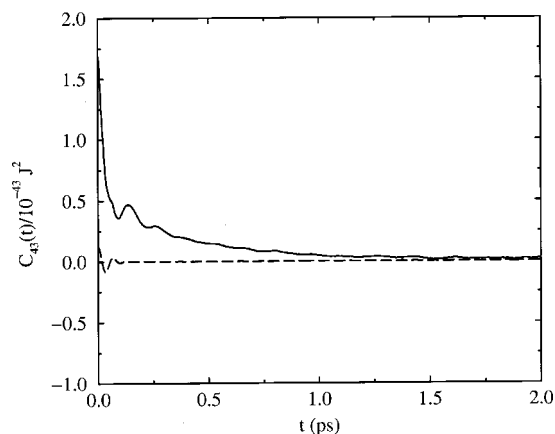


FIG. 3. $C_{43}(t)$. The real part is shown by the solid line and the imaginary part by the dashed line.

libration with a period of about 100 fs. Both linear velocity TCFs show a hindered translation with a period of about 140 fs. Thus we can identify the 70 fs oscillation of the imaginary part in Fig. 3 as coming from the HOD libration (which makes sense since the Coriolis term involves only the HOD molecule), while the 130 fs oscillation in the real part is due to the hindered translations.

In Fig. 5 are shown $\hat{C}_{4j}(\omega)$ for each of the transitions. For clarity of presentation we have shown results only for positive frequency, even though (as discussed above) $\hat{C}_{ij}(\omega)$ are not even functions of frequency, and for some transitions (to states higher in energy than the initial state) the Fourier transforms need to be evaluated at negative frequency. There are several more or less general features. Following the peak at zero frequency there is a plateau from about 100 to 250 cm^{-1} . There is a peak (which may appear as a second plateau) that is centered at about 500 cm^{-1} . Finally, there is another plateau that extends to about 1500 cm^{-1} , which is followed by a nearly exponential decay. From the above time scales one can identify the origin of these features. But for an even more direct comparison, in Fig. 6 we show the Fourier transforms of the TCFs in Fig. 4. From these results we can identify the plateau from 100 to 250 cm^{-1} as arising from the hindered translations, and the peak–plateau at 500 cm^{-1} as arising from the librations for both molecules. Indeed, these identifications have been known for some time from both simulation and experiment.^{36,68–70} While we cannot show definitively what causes the final plateau, it would appear to arise from higher librational “overtone.” In summary then, our calculation shows that the T_1 relaxation of the OH stretch fundamental is dominated by the transition to the bend overtone, and that the energy released in this process (about 350 cm^{-1}) goes into librations.

As Eq. (20) shows, the perturbation V is composed of several different contributions. It is then interesting to look at the various terms that contribute to T_1 . For simplicity, we will focus on k_{43} , the rate constant for the transition to the bend overtone. Table II breaks this rate constant into contributions arising from the potential (H_{int}), centrifugal, and Coriolis terms, and all of the cross terms. We see that the centrifugal terms contribute little to the overall rate constant. On

TABLE I. Transition rate constants from the OH stretch fundamental ($l=4$) to vibrational state j .

State	j	ω_{4j} (cm^{-1})	k_{4j} (s^{-1})
2nd Bend overtone ($ 030\rangle$)	6	−1121	1.51×10^7
Bend/OD stretch combination ($ 110\rangle$)	5	−661	6.43×10^8
Bend overtone ($ 020\rangle$)	3	343	2.46×10^{11}
OD stretch fundamental ($ 100\rangle$)	2	836	3.32×10^{10}
Bend fundamental ($ 010\rangle$)	1	1829	7.22×10^{10}
Ground state ($ 000\rangle$)	0	3338	1.55×10^{10}

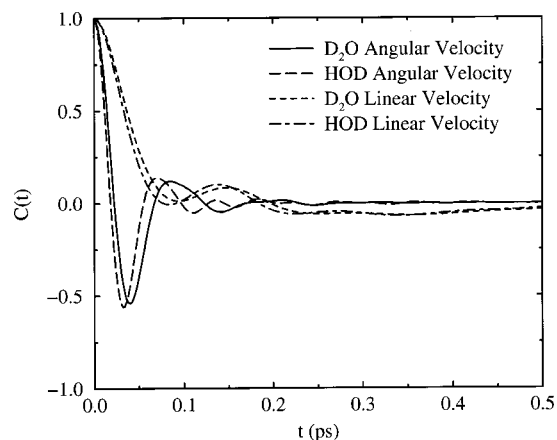


FIG. 4. Linear and angular velocity time-correlation functions for both the HOD and D₂O molecules.

the other hand the Coriolis contributions are in principle significant, but it turns out that in this case the potential–Coriolis and Coriolis–Coriolis terms nearly cancel. Table III further breaks up the potential contribution into the Lennard-Jones and Coulomb terms. It is not entirely surprising to find that the weaker Lennard-Jones interactions are dominated by the stronger Coulomb forces.

As explained earlier, V is expressed as a Taylor series in the normal mode coordinates and momenta. Table IV breaks k_{43} into contributions from the terms in this series, and their cross terms. Here q_s corresponds to all terms linear in the coordinates, $q_s q_{s'}$ corresponds to all terms quadratic in the coordinates (including those with $s = s'$), etc. The terms involving p_s are from the Coriolis interaction. If the potential were very anharmonic then only the linear terms would be important. On the other hand, if the potential were nearly harmonic, to make a transition from one quantum of OH stretch to two quanta of bend, the important term would be the diagonal one involving $q_2^2 q_3$. In fact, nearly all terms in the table are comparable, showing that neither of these limits is realized. There is no physical reason why terms of quartic order or higher should make appreciable contributions, and

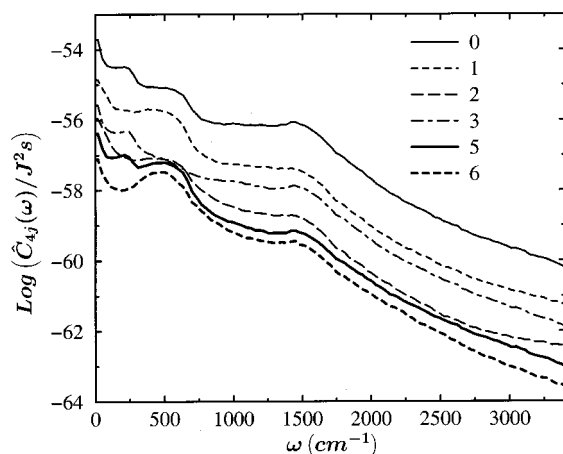


FIG. 5. Fourier transforms of $C_{4j}(t)$ for the transitions from the OH stretch fundamental to state j .

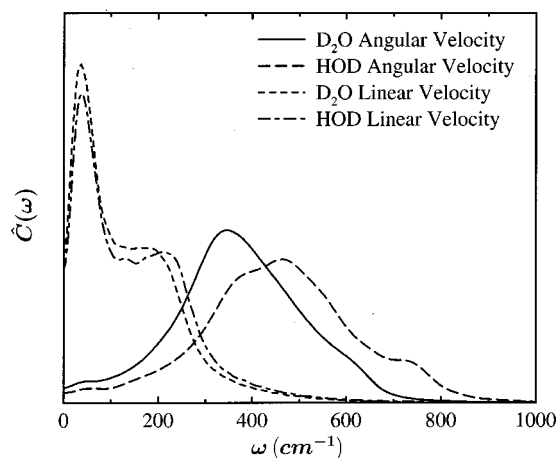


FIG. 6. Fourier transforms of linear and angular velocity time-correlation functions for both the HOD and D₂O molecules.

so we feel comfortable truncating the expansion after third order.

Next we calculated T_1 for the OD stretch fundamental. In order to do so the iterative procedure described at the beginning of the section was implemented again, this time for $l=2$. As a result both the system and bath Hamiltonians differ from when $l=4$ (the OH fundamental). As before, the bath Hamiltonian is used for the molecular-dynamics simulation and the eigenvalues of the system Hamiltonian lead to a set of transition frequencies, which are somewhat different, for example, from those obtained for $l=4$. These transition frequencies are given in Table V, along with the resulting rate constants. The calculated T_1 is 18 ps. In this case the transition rate to the bend fundamental dominates, while the transition to the ground state also contributes significantly.

The calculation was repeated once again for the bend fundamental ($l=1$), and the results are given in Table VI. T_1 in this case is 220 fs, and the relaxation is completely dominated by a direct transition to the ground state.

To explain the large differences among the three relaxation times, we note that for a given pair of states the rate constant results from a delicate interplay between $\hat{C}_{lj}(\omega_{lj})$ and the quantum correction factor, $Q(\omega_{lj})$. Since the general features of $\hat{C}_{lj}(\omega)$ are roughly the same for all l and j , variations come primarily from its initial value and the frequency at which it is evaluated. This initial value is determined by matrix elements of products of the vibrational coordinates and momenta. As such, if the vibrational modes were only weakly anharmonic and the expansion of V were truncated at

TABLE II. Decomposition of the rate constant k_{43} (for the transition from the OH stretch fundamental to the bend overtone).

Contribution	Rate (s^{-1})
Pot–Pot	2.37×10^{11}
Pot–Cent	8.17×10^9
Pot–Cor	-7.07×10^{10}
Cent–Cent	3.03×10^9
Cent–Cor	-2.66×10^9
Cor–Cor	8.17×10^{10}

TABLE III. Decomposition of the potential contribution to the rate constant k_{43} .

Contribution	Rate (s ⁻¹)
Coulomb–Coulomb	2.07×10^{11}
Coulomb–LJ	2.83×10^{10}
LJ–LJ	2.47×10^9

first order, the transitions that are harmonically “allowed,” that is, those that change one of the three quantum numbers by one, would have much greater values for $\hat{C}_{lj}(0)$. Although the real situation is much more complicated, $\hat{C}_{lj}(0)$ does tend to be larger for these transitions. While the nearly exponential decay of $\hat{C}_{lj}(\omega)$ for large frequency favors transitions at lower frequency, the quantum correction factor favors higher frequencies. It also greatly favors positive over negative frequencies.

The bend vibration is more harmonic than either of the stretches. As such, the matrix elements favor transitions from the bend fundamental to states where a single quantum number differs by one, namely the ground state, the bend overtone, and either of the bend–stretch combinations. These transitions are all at relatively large frequencies, so the quantum correction factor greatly diminishes the upward transitions, while serving to amplify the rate of the transition to the ground state. What makes this rate particularly large is that its frequency is about 1500 cm^{-1} , at which point $\hat{C}_{10}(\omega)$ has not decayed that far. For the OH fundamental, however, the one-quantum transition is to the ground state, which is 3400 cm^{-1} lower in energy. At this frequency, $\hat{C}_{40}(\omega)$ is well in the regime of its nearly exponential decay, leading to a relatively small rate. Nonetheless, the overall relaxation of the OH stretch fundamental is still fairly fast since there is an energy level available only 350 cm^{-1} below. The initial value of $\hat{C}_{43}(\omega)$ for this transition may not be particularly large, but it has not decayed much at all at such a low frequency. In the case of relaxation from the OD stretch fundamental, the two transitions that change the quantum numbers by one are those to the ground state and the combination band. The transition to the ground state is at too high of a frequency to have a particularly large rate. While the transition to the combination band is at about -1500 cm^{-1} , which places it before the exponential decay of $\hat{C}_{lj}(\omega)$, it is an upward transition. Accordingly, the rate is not very large due to the quantum correction factor. In addition, the OD relaxation does not benefit from the presence of a nearby lower energy level (the nearest level at lower energy is the bend

TABLE V. Transition rate constants from the OD stretch fundamental ($l=2$) to vibrational state j .

State	j	$\omega_{2j} \text{ (cm}^{-1}\text{)}$	$k_{2j} \text{ (s}^{-1}\text{)}$
2nd Bend overtone ($ 030\rangle$)	6	-1944	3.00×10^3
Bend/OD stretch combination ($ 110\rangle$)	5	-1485	4.66×10^9
OH stretch fundamental ($ 001\rangle$)	4	-911	4.25×10^8
Bend overtone ($ 020\rangle$)	3	-491	4.29×10^9
Bend fundamental ($ 010\rangle$)	1	984	3.95×10^{10}
Ground state ($ 000\rangle$)	0	2482	7.27×10^9

fundamental about 1000 cm^{-1} away). Thus, in this case the relaxation process consists of a sum of modest rates, yielding a relatively slow result.

V. DISCUSSION AND CONCLUSION

As described in the previous section, for HOD in D₂O we have calculated the relaxation times for the fundamentals of the OH stretch, the OD stretch, and the bend. The dominant path by which energy leaves the OH stretch fundamental is transfer to the bend overtone, the OD stretch fundamental relaxes primarily by way of the bend fundamental, and the bend fundamental goes directly to the ground state. The calculated relaxation times for these three excitations are 2.7 ps, 18 ps, and 220 fs, respectively. (The experimental T_1 for the OH stretch is about 1 ps, and the relaxation times for the other states of HOD in D₂O have not been measured.) Several years ago Rey and Hynes studied this problem quite extensively and came to similar conclusions.³⁶ They calculated a T_1 of 7.7 ps for the OH stretch fundamental, with excitation of the bend overtone as the dominant step in the relaxation pathway. For the OD stretch fundamental they find a T_1 of 23.8 ps, and the direct transition to the ground state dominates (whereas we find the dominant pathway is to the bend fundamental). Finally, for the bend fundamental, they calculated a T_1 of 1.6 ps. As mentioned in the Introduction, while our theoretical approach is very similar in spirit to that of Rey and Hynes, there are a number of significant differences. We are surprised that these differences lead to a decrease of the calculated lifetime, for example for the OH stretch, by only a factor of about 3 (although there is a factor of 7 decrease for the bend fundamental). We have analyzed this situation in some detail, and find in fact that many different factors, some varying between our two calculations by over an order of magnitude, conspire to produce results that are more similar than different.

One of the differences between our two calculations is that RH used a flexible solvent model, whereas we used a

TABLE IV. Decomposition of the rate constant k_{43} in terms of the expansion order.

	q_s	$q_s q_{s'}$	$q_s q_{s'} q_{s''}$	$p_s q_{s'}$	$p_s q_{s'} q_{s'}$
q_s	6.71×10^{10}	7.35×10^{10}	2.02×10^{10}	-1.67×10^{10}	5.30×10^8
$q_s q_{s'}$		5.72×10^{10}	2.45×10^{10}	-4.80×10^{10}	1.53×10^9
$q_s q_{s'} q_{s''}$			5.29×10^9	-1.11×10^{10}	3.54×10^8
$p_s q_{s'}$				8.71×10^{10}	-5.54×10^9
$p_s q_{s'} q_{s'}$					8.82×10^7

TABLE VI. Transition rate constants from the bend fundamental ($l=1$) to vibrational state j .

State	j	ω_{1j} (cm ⁻¹)	k_{1j} (s ⁻¹)
2nd Bend overtone ($ 030\rangle$)	6	-2922	3.47×10^3
Bend/OD stretch combination ($ 110\rangle$)	5	-2497	5.07×10^4
OH stretch fundamental ($ 001\rangle$)	4	-1908	2.11×10^6
Bend overtone ($ 020\rangle$)	3	-1472	9.03×10^9
OD stretch fundamental ($ 100\rangle$)	2	-1015	2.27×10^8
Ground state ($ 000\rangle$)	0	1494	4.45×10^{12}

rigid solvent. We were guided in this regard by the results of RH: That the OH stretch fundamental relaxation was dominated by transition to the bend overtone, and, for example, the transition rate to the bend fundamental was smaller by over two orders of magnitude.³⁶ The energy gaps for these two transitions are 530 and 1980 cm⁻¹, respectively, (RH) and 343 and 1829 cm⁻¹ (this work). The important point is that the gap for the first transition is much smaller than the lowest frequency intramolecular vibration of the D₂O solvent (which is the bend at about 1200 cm⁻¹), implying that this bend would not be an important accepting mode, and so it should not make any substantial difference if the solvent is treated flexibly or not. On the other hand, the energy gap for the second transition is higher than the bend frequency, so that in principle relaxation could involve excitation of one quantum of solvent bend. However, the RH results showed that even with a flexible solvent the transition to the bend fundamental is negligible. Thus we believed that, at least for the OH stretch fundamental T_1 , it was not important to use a flexible solvent.

Looking at the entries in Table I, however, we see that in fact for our model the transition rate to the bend fundamental is only a factor of about 3.5 smaller than the dominant rate constant for relaxation to the bend overtone (and two orders of magnitude *larger* than that found by RH). The implication is that for our model, if we included solvent vibrations we might find that this pathway to the bend fundamental competes favorably with or even dominates the transition to the bend overtone. Likewise, even the direct transition to the ground state could become considerably more important. In either case the overall rate would increase, possibly bringing the theoretical number into better agreement with experiment. For relaxation from the other states the argument for including solvent vibration is even more compelling: Near-resonant energy transfer from the OD stretch and bend fundamentals to OD stretches and the bend of the D₂O solvent, respectively, will likely be very important. Therefore, we are in the process of repeating these calculations using a flexible solvent, and hope to have results available soon. We also intend to extend these results by calculating the frequency³¹ and temperature²⁹ dependence of the T_1 following OH stretch excitation, and to calculate the T_1 following OD excitation of HOD in H₂O.³⁵

The above discussion focuses primarily on the fate of the HOD molecule. On the other hand it is equally important to understand what intramolecular and intermolecular solvent modes are excited by the relaxation process. There is a suggestion that following OH excitation the energy flows into

excitations of the hydrogen bond itself.²⁹ We note that this is not necessarily incompatible with our results, in that for any relaxation pathway, an amount of excess energy smaller than the lowest intramolecular solvent frequency (in this case about 1200 cm⁻¹ for the the bend) will most likely go into one or more quanta of librations and/or hindered translations. Thus this excess energy would most likely go directly into HOD-D₂O hydrogen-bond excitations (although it would certainly not be enough energy to break the hydrogen bond^{29,71,72}). Very recent infrared pump/Raman probe experiments of Dlott and co-workers³⁴ show that following OH excitation both solvent stretch and bend modes are excited on the 1 ps time scale, and that the bend excitations cannot be generated solely from relaxation of the solvent stretch. If in the end (after we include solvent vibrations) it turns out that the transition to the HOD bend fundamental is important, this will likely imply concomitant excitation of solvent bend modes, consistent with these Raman probing experiments. In any case, at this point it is unclear if these hydrogen-bond or solvent-bend excitations occur during the first relaxation step along the pathway, or rather occur during subsequent relaxation steps from intermediate states. To provide more insight into these questions, after we include solvent vibrations, we intend to map out the entire relaxation process of the HOD molecule by solving the vibrational master equation. This should provide some important information about which solvent modes are being excited, and when.

There is one aspect of this work that bothers us: the charges on the HOD molecule are independent of vibrational coordinates. If one considers the potential of Polyansky *et al.*⁴⁰ for the gas-phase HOD molecule, one can assign charges in order to get the correct experimental dipole moment of HOD in its vibrational ground state.⁷³ If one then uses these same charges to calculate the dipole moment for the OH stretch fundamental, the difference between these two values is too large (compared to experiment) by a factor of 4.4.⁷³ Within a point charge model, then, to reproduce experiment for the isolated molecule it would be important to let the charges themselves depend on the vibrational coordinates. Of course our model is for HOD in solution, and the charges we assigned to HOD are not the gas-phase charges anyway. And it may turn out that the constant charge approximation works better in solution. (One does not have good experimental numbers for the dipole moment of a water molecule in the neat liquid, much less as a function of vibrational state!) Nonetheless, it is perhaps something to worry about. Preliminary attempts by us to include this coordinate dependence were not successful, but we intend to pursue the matter further.

This paper is the first in a series on the vibrational spectroscopy of HOD in liquid D₂O. Our overall goal is to describe theoretically and provide insight into a whole set of recent exciting experiments on this system. Thus while the present paper does not present dramatically different results or mechanisms from those of Rey and Hynes,³⁶ it does set the stage for our subsequent work, by establishing a reasonably accurate and flexible theoretical framework. In particular, we believe the flexibility inherent in our self-consistent renormalization procedure is critical for performing satisfac-

tory calculations of infrared line positions, and the vibrational Stokes shift. Paper II⁶⁰ of the series presents a calculation of the infrared line shapes for the various modes of HOD, and a calculation of the vibrational Stokes shift for the OH stretching mode.⁵⁴ For the line shape calculation we will use the values of T_1 determined herein. Paper III⁷⁴ discusses the connection between transient hole burning^{30,32} and rotational anisotropy⁷⁵ experiments, and hydrogen bond making and breaking dynamics. Paper IV⁷⁶ will focus on trying to understand very recent two- and three-pulse vibrational photon echo experiments.^{77,78} In all of this work we will use the Hamiltonian and approach described herein. We believe that taken together, all these recent experiments, along with theory, provide a reasonably complete picture of the dynamics of liquid water.

ACKNOWLEDGMENTS

We are very grateful to our colleague Professor Ned Sibert for assistance in setting up, understanding, and diagonalizing the Hamiltonian for the isolated HOD molecule, and for a critical reading of the manuscript. The authors also thank Dr. Andrei Piryatinski for helpful discussions. We are grateful for support from the National Science Foundation, through Grant Nos. CHE-9816235 and CHE-0132538.

- ¹D. Eisenberg and W. Kauzmann, *The Structure and Properties of Water* (Oxford University Press, New York 1969).
- ²*Water: A Comprehensive Treatise*, edited by F. Franks, Vol. 1 (Plenum, New York, 1972).
- ³*Water and Aqueous Solutions: Structure, Thermodynamics and Transport Processes*, edited by R. A. Horne (Wiley, New York, 1972).
- ⁴*The Hydrogen Bond: Recent Developments in Theory and Experiments*, edited by P. Schuster, G. Zundel, and C. Sandorfy (North-Holland, Amsterdam, 1976), Vols. 1–3.
- ⁵A. K. Soper, F. Bruni, and M. A. Ricci, *J. Chem. Phys.* **106**, 247 (1997).
- ⁶A. K. Soper, *Chem. Phys.* **258**, 121 (2000).
- ⁷C. Rønne, L. Thrane, P.-O. Åstrand, A. Wallqvist, K. V. Mikkelsen, and S. R. Keiding, *J. Chem. Phys.* **107**, 5319 (1997).
- ⁸J. C. Hindman, A. J. Zielen, A. Svirmicks, and M. Wood, *J. Chem. Phys.* **54**, 621 (1971).
- ⁹J. Ropp, C. Lawrence, T. C. Farrar, and J. L. Skinner, *J. Am. Chem. Soc.* **123**, 8047 (2001).
- ¹⁰R. M. Whitnell, K. R. Wilson, and J. T. Hynes, *J. Chem. Phys.* **96**, 5354 (1992).
- ¹¹J. C. Owrrsky, D. Raftery, and R. M. Hochstrasser, *Annu. Rev. Phys. Chem.* **45**, 519 (1994).
- ¹²M. Li, J. Owrrsky, M. Sarisky, J. P. Culver, A. Yodh, and R. M. Hochstrasser, *J. Chem. Phys.* **98**, 5499 (1993).
- ¹³M. Ferrario, M. L. Klein, and I. R. McDonald, *Chem. Phys. Lett.* **213**, 537 (1993).
- ¹⁴D. A. Yarne, M. E. Tuckerman, and M. L. Klein, *Chem. Phys.* **258**, 163 (2000).
- ¹⁵A. Morita and S. Kato, *J. Chem. Phys.* **109**, 5511 (1998).
- ¹⁶C. M. Cheatum, M. M. Heckscher, D. Bingemann, and F. F. Crim, *J. Chem. Phys.* **115**, 7086 (2001).
- ¹⁷A. Charvat, J. Absmann, B. Abel, D. Schwarzer, K. Henning, K. Luther, and J. Troe, *Phys. Chem. Chem. Phys.* **3**, 2230 (2001).
- ¹⁸K. Sekiguchi, A. Shimojima, and O. Kajimoto, *Chem. Phys. Lett.* **356**, 84 (2002).
- ¹⁹D. J. Myers, M. Shigeiwa, M. D. Fayer, and B. J. Cherayil, *J. Phys. Chem. B* **104**, 2402 (2000).
- ²⁰S. A. Egorov and J. L. Skinner, *J. Chem. Phys.* **112**, 275 (2000).
- ²¹H. Graener, R. Zürl, and M. Hofmann, *J. Phys. Chem. B* **101**, 1745 (1997).
- ²²H. Graener, T. Patzlaff, N. Kadarisman, and G. Seifert, *Chem. Phys. Lett.* **348**, 403 (2001).
- ²³N. E. Levinger, P. H. Davis, and M. D. Fayer, *J. Chem. Phys.* **115**, 9352 (2001).
- ²⁴E. L. Sibert and R. Rey, *J. Chem. Phys.* **116**, 237 (2001).
- ²⁵J. A. Poulsen, T. M. Nymand, and S. R. Keiding, *Chem. Phys. Lett.* **343**, 581 (2001).
- ²⁶K. L. Vodopyanov, *J. Chem. Phys.* **94**, 5389 (1991).
- ²⁷H. Graener, G. Seifert, and A. Laubereau, *Phys. Rev. Lett.* **66**, 2092 (1991).
- ²⁸S. Woutersen, U. Emmerichs, H.-K. Nienhuys, and H. J. Bakker, *Phys. Rev. Lett.* **81**, 1106 (1998).
- ²⁹H.-K. Nienhuys, S. Woutersen, R. A. van Santen, and H. J. Bakker, *J. Chem. Phys.* **111**, 1494 (1999).
- ³⁰G. M. Gale, G. Gallot, F. Hache, N. Lascoux, S. Bratos, and J.-Cl. Leicknam, *Phys. Rev. Lett.* **82**, 1068 (1999).
- ³¹G. M. Gale, G. Gallot, and N. Lascoux, *Chem. Phys. Lett.* **311**, 123 (1999).
- ³²R. Laenen, C. Rauscher, and A. Laubereau, *Phys. Rev. Lett.* **80**, 2622 (1998).
- ³³R. Laenen, C. Rauscher, and A. Laubereau, *J. Phys. Chem. B* **102**, 9304 (1998).
- ³⁴J. C. Deak, S. T. Rhea, L. K. Iwaki, and D. D. Dlott, *J. Phys. Chem. A* **104**, 4866 (2000).
- ³⁵M. F. Kropman, H.-K. Nienhuys, S. Woutersen, and H. J. Bakker, *J. Phys. Chem. A* **105**, 4622 (2001).
- ³⁶R. Rey and J. T. Hynes, *J. Chem. Phys.* **104**, 2356 (1996).
- ³⁷D. W. Oxtoby, *Adv. Chem. Phys.* **47** (Part 2), 487 (1981).
- ³⁸M. G. Sceats and S. A. Rice, *J. Chem. Phys.* **71**, 973 (1979).
- ³⁹K. Toukan and A. Rahman, *Phys. Rev. B* **31**, 2643 (1985).
- ⁴⁰O. L. Polyansky, P. Jensen, and J. Tennyson, *J. Chem. Phys.* **105**, 6490 (1996).
- ⁴¹L. Frommhold, *Collision-induced absorption in gases, Vol. 2 of Cambridge Monographs on Atomic, Molecular, and Chemical Physics*, 1st ed. (Cambridge University Press, England, 1993).
- ⁴²J. S. Bader and B. J. Berne, *J. Chem. Phys.* **100**, 8359 (1994).
- ⁴³D. Rostkier-Edelstein, P. Graf, and A. Nitzan, *J. Chem. Phys.* **107**, 10470 (1997).
- ⁴⁴J. L. Skinner, *J. Chem. Phys.* **107**, 8717 (1997).
- ⁴⁵S. A. Egorov and J. L. Skinner, *Chem. Phys. Lett.* **293**, 469 (1998).
- ⁴⁶S. A. Egorov, K. F. Everitt, and J. L. Skinner, *J. Phys. Chem. A* **103**, 9494 (1999).
- ⁴⁷S. A. Egorov, E. Rabani, and B. J. Berne, *J. Phys. Chem. B* **103**, 10978 (1999).
- ⁴⁸J. L. Skinner and K. Park, *J. Phys. Chem. B* **105**, 6716 (2001).
- ⁴⁹P. A. Egelstaff, *Adv. Phys.* **11**, 203 (1962).
- ⁵⁰P. Schofield, *Phys. Rev. Lett.* **4**, 239 (1960).
- ⁵¹K. F. Everitt, S. A. Egorov, and J. L. Skinner, *Chem. Phys.* **235**, 115 (1998).
- ⁵²K. F. Everitt and J. L. Skinner, *J. Chem. Phys.* **110**, 4467 (1999).
- ⁵³K. F. Everitt, J. L. Skinner, and B. M. Ladanyi, *J. Chem. Phys.* **116**, 179 (2002).
- ⁵⁴S. Woutersen and H. J. Bakker, *Phys. Rev. Lett.* **83**, 2077 (1999).
- ⁵⁵E. B. Wilson Jr., J. C. Decius, and P. C. Cross, *Molecular vibrations* (Dover, New York, 1980).
- ⁵⁶J. K. G. Watson, *Mol. Phys.* **15**, 479 (1968).
- ⁵⁷B. T. Darling and D. M. Dennison, *Phys. Rev.* **57**, 128 (1940).
- ⁵⁸W. S. Benedict, N. Gailar, and E. K. Plyler, *J. Chem. Phys.* **24**, 1139 (1956).
- ⁵⁹W. L. Jorgensen, J. Chandrasekhar, J. D. Madura, R. W. Impey, and M. L. Klein, *J. Chem. Phys.* **79**, 926 (1983).
- ⁶⁰C. P. Lawrence and J. L. Skinner, *J. Chem. Phys.* (to be published).
- ⁶¹M. P. Allen and D. J. Tildesley, *Computer Simulation of Liquids* (Clarendon, Oxford, 1987).
- ⁶²S. A. Egorov and J. L. Skinner, *J. Chem. Phys.* **105**, 7047 (1996).
- ⁶³J. L. Skinner, S. A. Egorov, and K. F. Everitt, "Vibrational energy relaxation in liquids and supercritical fluids," in *Ultrafast Infrared and Raman Spectroscopy*, edited by M. Fayer (Marcel Dekker, New York, 2001), p. 675.
- ⁶⁴D. J. Adams and G. S. Dubey, *J. Comput. Phys.* **72**, 156 (1987).
- ⁶⁵M. Svanberg, *Mol. Phys.* **92**, 1085 (1997).
- ⁶⁶F. J. Harris, *Proc. IEEE* **66**, 51 (1978).
- ⁶⁷W. H. Press, B. P. Flannery, S. A. Teukolsky, and W. T. Vetterling, *Numerical Recipes* (Cambridge University Press, Cambridge, 1986).
- ⁶⁸E. W. Castner, Jr., Y. J. Chang, Y. C. Chu, and G. E. Walrafen, *J. Chem. Phys.* **102**, 653 (1995).

- ⁶⁹J. T. Kindt and C. A. Schmittenmaer, J. Chem. Phys. **106**, 4389 (1997).
- ⁷⁰D. M. Carey and G. M. Korenowski, J. Chem. Phys. **108**, 2669 (1998).
- ⁷¹J. T. Hynes and R. Rey, "Coulomb force and intramolecular energy flow effects for vibrational energy transfer for small molecules in polar solvents," in *Ultrafast Infrared and Raman Spectroscopy*, edited by M. D. Fayer (Markel Dekker, New York, 2001), p. 593.
- ⁷²A. Staib and J. T. Hynes, Chem. Phys. Lett. **204**, 197 (1993).
- ⁷³S. L. Shostak and J. S. Muentner, J. Chem. Phys. **94**, 5883 (1991).
- ⁷⁴C. P. Lawrence and J. L. Skinner, J. Chem. Phys. (to be published).
- ⁷⁵S. Woutersen, U. Emmerichs, and H. J. Bakker, Science **278**, 658 (1997).
- ⁷⁶A. Piryatinski, C. P. Lawrence, and J. L. Skinner (unpublished).
- ⁷⁷J. Stenger, D. Madsen, P. Hamm, E. T. J. Nibbering, and T. Elsaesser, Phys. Rev. Lett. **87**, 027401 (2001).
- ⁷⁸J. Stenger, D. Madsen, P. Hamm, E. T. J. Nibbering, and T. Elsaesser, J. Phys. Chem. A **106**, 2341 (2002).